Role of graphene inter layer on the formation of the MoS_2-CZTS interface during growth

Manoj Vishwakarma, Narayana Thota, Olesia Karakulina, Joke Hadermann, and B. R. Mehta

Citation: AIP Conference Proceedings **1953**, 100064 (2018); doi: 10.1063/1.5033000
View online: https://doi.org/10.1063/1.5033000
View Table of Contents: http://aip.scitation.org/toc/apc/1953/1
Published by the American Institute of Physics

Role of Graphene Inter Layer on the Formation of the MoS_2 - CZTS Interface during Growth

Manoj Vishwakarma[1a], Narayana Thota[1], Olesia Karakulina[2], Joke Hadermann[2] and B.R. Mehta[1*]

1Thin Film Lab, Dept. of Physics, IIT DELHI New Delhi-110016, India
2EMAT, University of Antwerp, Groenenborgerlaan 171, B-2020 Belgium

[a)] Corresponding author: manojphyiitd@gmail.com

Abstract. The growth of MoS_2 layer near the Mo/CZTS interface during sulphurization process can have an impact on back contact cell parameters (series resistance and fill factor) depending upon the thickness or quality of MoS_2. This study reports the dependence of the thickness of interfacial MoS_2 layer on the growth of graphene at the interface between molybdenum back contact and deposited CZTS layer. The graphene layer reduces the accumulation of Zn/ZnS, Sn/SnO_2 and formation of pores near the MoS_2-CZTS interface. The use of graphene as interface layer can be potentially useful for improving the quality of Mo/MoS_2/CZTS interface.

INTRODUCTION

Cu_2ZnSnS_4 is a potential absorber material for next generation thin film solar cell devices. CZTS thin films have excellent properties and its constituents are earth abundant and non-toxic with a suitable electronic band gap (~1.4-1.5 eV) and high absorption coefficient ($\alpha > 10^4$ cm^{-1}) [1]. The Mo-CZTS interface properties are crucial to cell parameters (current density, open circuit voltage (V_{OC}), fill factor, series resistance and shunt resistance) [2]. Lower V_{OC} is reported due to high carrier recombination losses at intra-grain defects between CZTS and Mo-back contact interface layer (MoS_2) [3]. The MoS_2 layer formed during annealing can also increase the series resistance of device thus reducing the V_{OC} [4-5-6]. A recent study has shown that MoS_2 layer at Mo/CZTS interface increases V_{OC} and fill factor because of diffusion of Mo into the CZTS near the interface [7]. The optimized thickness of the p-MoS_2 between Mo and CZTS is important for improved device performance [3]. The thickness of MoS_2 increases with increase in temperature (500°-600°C) and thickness of CZTS layer [7]. In the present work, graphene is deposited on Mo-coated glass substrate followed by sputter growth of CZTS thin film and post deposition annealing. The effect of graphene layer on the growth of MoS_2 interface layer is investigated.

EXPERIMENTAL

CZTS thin films were synthesized by sputtering from precursor targets Cu, ZnS and SnS on Mo-coated glass (Sample A) and on Mo coated glass substrate with graphene flakes dispersed on top (Sample B). The single layer graphene flakes are deposited by spin coating of solution consisting of SLG and DI water (10 mg/ml). As deposited CZTS thin films were sulphurized in a rapid thermal annealing furnace (RTA) for 20 minutes at ~ 540°C resulting in the formation of CZTS thin films having kesterite phase. The detailed cross-sectional TEM studies have been carried out to study the growth of MoS_2 interfacial layer.

2nd International Conference on Condensed Matter and Applied Physics (ICC 2017)
AIP Conf. Proc. 1953, 100064-1–100064-4; https://doi.org/10.1063/1.5033000
Published by AIP Publishing. 978-0-7354-1648-2/$30.00

RESULTS AND DISCUSSION

XRD and Raman spectra of CZTS layer are shown in Fig.1 (sample A). The XRD spectrum reveals the kesterite phase along with minor SnO_2 phase (Fig 1.a). Raman spectrum of Mo + Graphene sample shows peaks at 1350 cm^{-1} and 1585 cm^{-1} which are attributed to D and G peaks of graphene (Fig .1c). The Raman peaks at 337 cm^{-1} and 286 cm^{-1} observed for sample A and sample B are attributed to kesterite phase (Fig 1.b).

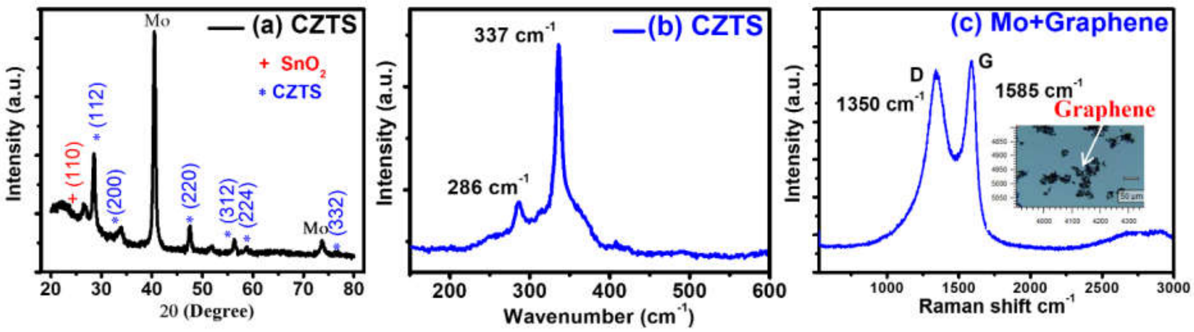

FIGURE 1. (a) XRD, (b) Raman spectra of sulphurized samples showing kesterite phase. (c) Raman spectra of Mo+graphene substrate used to deposited sample B (Inset image showing the dispersed flakes of graphene on Mo coated glass substrate).

The cross-sectional TEM analysis is carried out to study the effect of the presence of graphene on MoS_2 growth. The HAADF-STEM image of CZTS/MoS_2/Mo interface of sample A is shown in Fig. 2 (a). Mixed maps of Cu, Zn, Sn and Mo, S are shown in Fig.2 (b) and (c). In sample A, Zn and Sn are segregated more along with S in comparison to other constituent Cu. The accumulation of Zn along with S indicates the formation of ZnS secondary phase. At the interface between CZTS and Mo of the sample A, a lattice plane structure of MoS_2 phase can be seen in Fig. 3(a). The lattice inter-planer distance in sample A is ~ 6 Å, which is in agreement with literature data of MoS_2 (6.16 Å, ICSD 95569). This MoS_2 layer in sample A is attached to the Mo-surface (MoS_2-Mo interface) without any pores, but at CZTS-Mo interface ~10 nm pores can be observed (black spots in Fig.2 c). For sample B, the HAADF-STEM image shown in Fig.2 (d) represents Mo/MoS_2/CZTS interface, where, the region was marked by white arrows. The mixed map for Sample B shows Zn and Sn are rich in concentration in comparison to Cu, near the CZTS/MoS_2 interface regions (Fig. 2 d-e). At this interface region (in sample B), layer growth of MoS_2 is also observed with lattice plane distance ~ 4-6 Å (Fig.3 (c), but no pores between Mo-MoS_2 and MoS_2-CZTS interface are observed (Fig.2 e-f). The concentrations of Mo and S corresponding to MoS_2 regions for sample A and B are estimated from the peak intensity corresponding to Mo and S, as shown in Fig. 3 (b) and (d). The Mo/S ratios estimated for sample A and sample B are 30/70 and 36.4/63.4 (in Atomic %), respectively. The TEM investigations show the thickness of the the MoS_2 layer for samples A (Mo+CZTS) and B (Mo+Graphene+ CZTS) to be 20-30 nm and 15-20 nm, respectively. The presence of graphene seems to result in the reduced thickness of MoS_2 layer on going from sample A to B. No pore like features are found close to the CZTS/MoS_2 interface for sample B because graphene have high thermal and mechanical stability, which can also result in reducing defects at the interface [8]. Due to its high thermal stability, the graphene can also reduce the segregation of constituents near the interface in suppression of secondary phases near the Mo/CZTS interface. Further, the graphene can be used as a controlling agent for MoS_2 layer thickness, which can result into reduction of series resistance for future PV devices.

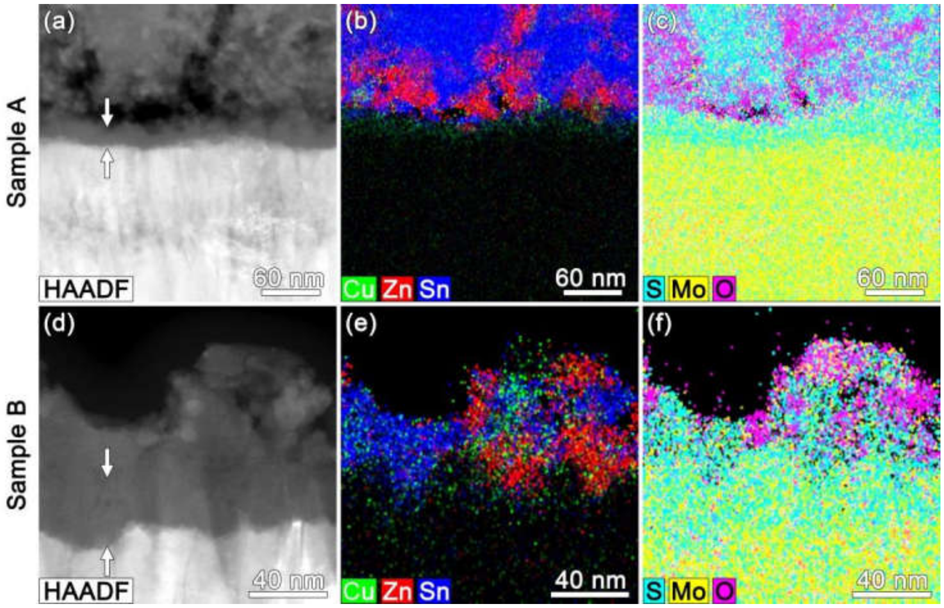

FIGURE 2. Mo/MoS$_2$/CZTS interface: (a) HAADF-STEM image, (b) mixed map of Cu, Zn and Sn, (c) mixed map of S and Mo of sample A. (d) HAADF-STEM image, (e) mixed map of Cu, Zn and Sn, (c) mixed map of S and Mo of sample B. The arrows marked the MoS$_2$ layer.

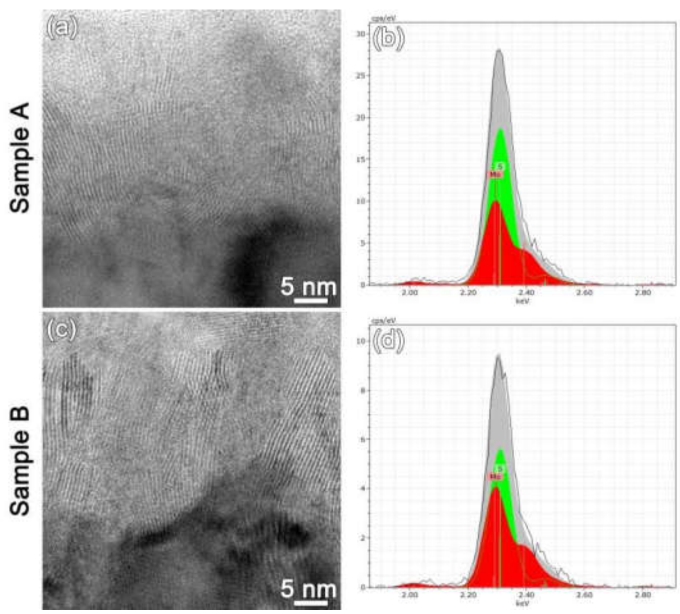

FIGURE 3. (a) HRTEM image of MoS$_2$/Mo interface of sample A, (b) EDX- spectrum of MoS$_2$ layer formed in sample A, (c) HRTEM image of MoS$_2$/Mo interface of sample B and (d) The EDX spectrum of MoS$_2$ layer in sample B.

CONCLUSIONS

The present work shows that the presence of a dispersed graphene layer deposited on Mo substrate can reduce the thickness of interfacial MoS$_x$ layer, even at high sulphurization temperatures required for CZTS(Se) thin film samples. Additionally it can also suppress the growth of secondary phases near the MoS$_2$/CZTS interface.

ACKNOWLEDGEMENT

The authors acknowledge support provided by DST project. M.V. acknowledges IIT Delhi for MHRD fellowship. Prof. B. R. Mehta acknowledges the support of the Schlumberger chair professorship.

REFERENCES

1. K. Ito and T. Nakazawa, Jpn. J. Appl. Phys. 27, 2094–2097 (1988).
2. E. M. Tennyson , J. L. Garrett , J. A. Frantz , J. D. Myers , R. Y. Bekele , J. S. Sanghera , J. N. Munday , and M. S. Leite, Adv. Energy Mater., Adv. Energy Mater. **5** (23), 1501142 (2015).
3. A. D. Adewoyin, M. A. Olopade and M. Chendo, Optik **133**, 122–131(2017).
4. H. Jiang, X. Wei, Y. Huang, X. Wang, A. Han, X. Liu, Z. Liu, and F. Meng, Jpn. J. Appl. Phys. **56**, 065502 (2017).
5. S. G. Haass, M. Diethelm, M. Werner, B. Bissig, Y. E. Romanyuk, and A. N. Tiwari, Adv. Energy Mater. **5** (18), 1500712 (2015).
6. K. J. Yang, J. H. Sim, B. Jeon, D. H. Son, D. H. Kim, S. J. Sung, D. K. Hwang, S. Song, D. B. Khadka, J. H. Kim, and J. K. Kang, Prog. Photovoltaics **23**, 862 (2015).
7. G. K. Dalapati, S. Zhuk, S. M. Panah, A. Kushwaha, H. L. Seng, V. Chellappan, V. Suresh, Z. Su, S. K. Batabyal, C. C.Tan, A. Guchhait, L. H. Wong, T. K. S. Wong and S. Tripathy, Sci. Rep. **7**, 1350 (2017).
8. E. Singh and H. S. Nalwa, RSC Adv. **5**, 73575 (2015).